

# InP Coherent Receiver Chip with High Performance and Manufacturability for CFP2 Modules

Selina Farwell<sup>1</sup>, Pantelis Aivaliotis<sup>1</sup>, Yahong Qian<sup>1</sup>, Paul Bromley<sup>1</sup>, Roger Griggs<sup>2</sup>, Joseph Ng Yew Hoe<sup>2</sup>, Colin Smith<sup>2</sup>, Stephen Jones<sup>1</sup>.

<sup>1</sup> Oclaro Technology, Caswell, Towcester, Northamptonshire, NN12 8EQ, UK

<sup>2</sup> Oclaro Technology, Westfield Business Park, Long Road, Paignton Devon, TQ4 7AU, UK  
selina.farwell@oclaro.com

**Abstract:** We report an InP coherent receiver chip with the highest reported responsivity (0.15A/W) together with excellent RF bandwidth (32GHz) and 4x4 MMI width fabrication control ( $< \pm 60\text{nm}$  90% population) providing a highly manufacturable Rx for CFP2 modules.

**OCIS codes:** (250.3140) Integrated optoelectronic circuits; (230.5170) Photodiodes

## 1. Introduction

The widespread adoption of digital coherent technology has been aided in part by standardization of function and footprint of the key optical building blocks, including the modulator and integrated coherent receiver (ICR). Driven by requirements for wider deployment in metro networks using pluggable modules, there is though currently great interest in miniaturized ICRs which maintain established performance but with significantly reduced footprint. InP PICs offer an attractive option for ICR miniaturization and cost reduction, complementing InP based lasers and modulators, as it allows integration of high-speed waveguide photodetectors together with optical hybrid mixer in a very small footprint. 4x4 MMIs offer the most compact implementation of the critical hybrid mixer, but pose challenges in process control to maintain high performance over a wide wavelength range.

A key benefit of the high level of integration is that automated characterization can be performed on bars of chips, providing extensive data to guide design and fabrication. Here we report on design optimization aided by analysis of >4000 fabricated chips, demonstrating excellent responsivity, power balance and hybrid angle. In addition InP chip area is 40% that of previous implementations [1]. The PICs may be packaged in a micro ICR 25x12x5mm Figure 1, providing standardized functionality in CFP2 module footprint 107.5x41.5x12.4 mm.

## 2. 100G DP-QPSK Micro InP chip and receiver

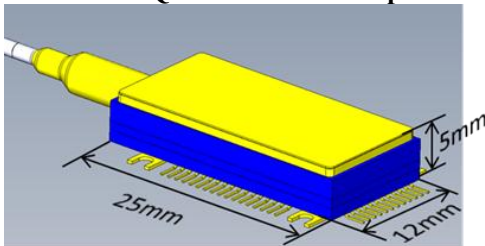


Figure 1 Micro ICR gold box package for CFP2 pluggable modules

In accordance with OIF implementation the micro ICR package contains the following functionality: signal and local oscillator (LO) fibre inputs, micro-optic signal VOA and MPD, power split for the LO and PBS split for the signal to demux the signal X and Y polarisations onto two separate InP chips, two dual TIAs and decoupling capacitors. The RF output signal output is provided in GSSG 100 $\Omega$  differential configuration over 4 channels.

Our chosen implementation of the micro coherent receiver chip (MCR) is shown in Figure 2. The chip comprises 2 inner device optical inputs for the signal and LO beams, spot size converters (SSC), mode cleaning filters, short input detectors and test features, 4x4 MMI 90degree hybrid, output bends, waveguide cross-overs (to re-order the I and Q channels), 4 waveguide photodetectors (PD), and 4 on-chip decoupling capacitors; all of this is contained on the InP chip with area 4mm<sup>2</sup>. On a 3inch InP wafer there are 620 die sites, highlighting the scalability and manufacturability of the InP platform. The chip also contains additional device test photodiode features (T\_PD\_L & T\_PD\_R) via the two outer input ports which are used to characterize the intrinsic PD responsivity etc.

## 3. Results

The waveguide PD responsivity is measured using T\_PD\_R and is shown across wavelength in Figure 3. At 1550nm

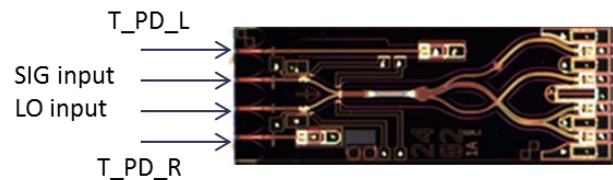


Figure 2 Single polarization 100G Micro Coherent Receiver InP Chip with monolithic 90degree hybrid and integrated waveguide photodetectors and capacitors, together with test photodetectors T\_PD\_L & T\_PD\_R; total size 1.2x3.33mm.

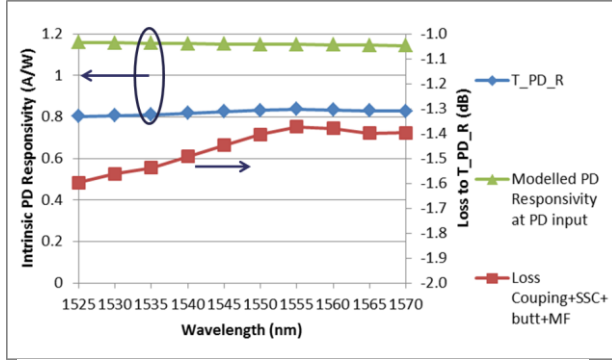


Figure 3 Photodetector, PD, responsivity 0.83A/W @ 1550nm

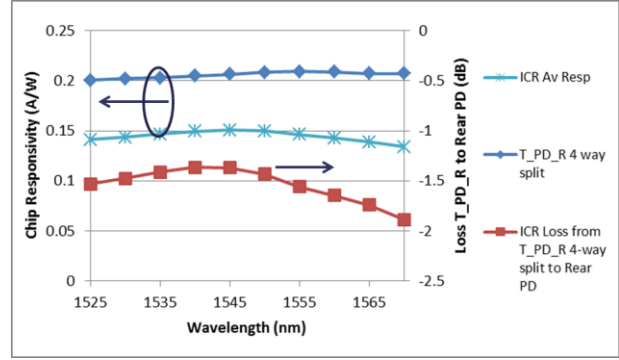


Figure 4 Intrinsic photodetector responsivity and on-chip losses 1.4dB @ 1550nm

the waveguide PD responsivity in this device is 0.83A/W. This PD responsivity includes the optical coupling, spot size converter and on-chip mode cleaning filter losses. This compares well with previously reported waveguide PD responsivity values. The modelled intrinsic waveguide responsivity, at the *input* to the PD at 1550nm is 1.15A/W. The difference between the modelled responsivity at the input to the PD and the measured waveguide PD responsivity provides an estimate of the coupling, SSC and mode filter loss combined of 1.4dB at 1550nm.

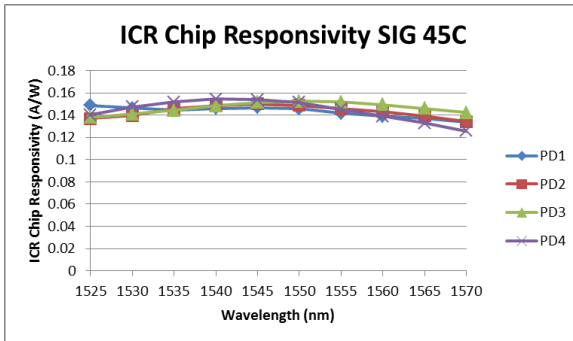


Figure 5 Micro ICR chip responsivity over wavelength for SIG input and for each output port. Average responsivity over PD 0.151A/W @ 1550nm

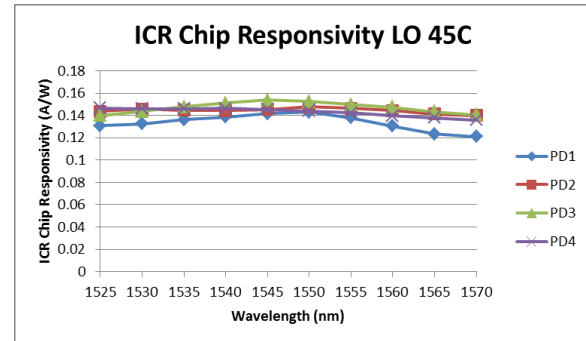


Figure 6 Micro ICR chip responsivity over wavelength for LO input and each output port. Average responsivity over PD 0.147A/W @ 1550nm

The full micro coherent receiver chip responsivity, inclusive of 6dB hybrid 90 and all waveguide loss, is reported in *Figure 5* and *Figure 6*, showing an average PD responsivity at 1550nm of 0.151A/W. These values are typical chip values across a wafer. This is the best full ICR chip responsivity in InP of which we are aware. The responsivity imbalance between waveguide detectors is <0.65dB and the I to Q phase offset from 90° is 2.2°.

Using the current waveguide PD conception, the maximum MCR rear PD responsivity for zero chip loss is 0.208A/W @ 1550nm, *Figure 4*. The actual ICR responsivity of 0.15A/W shows that the on-chip losses from after the input mode filter through 4x4 MMI, output bends, waveguide cross-overs at 1550nm, sum to only 1.4dB. This comprises mainly the loss from the two waveguide cross-overs per MMI output port of ~0.6dB, the residual waveguide propagation loss and sidewall scattering losses. In separate trials we have demonstrated lower loss in compatible InP waveguides, which should enable improved MCR chip responsivity. Using test PD, T\_PD\_L compared with responsivity of T\_PD\_R, the waveguide loss can be estimated as 1-3dB/cm over the C-Band.

Several MMI designs have been fabricated with the aim of reducing the wavelength dependence of the excess loss over wavelength. For a general interference MMI with ideal width centred in the C-Band, the 4x4 MMI can be miniaturised to  $L < 250\mu\text{m}$  and excess loss reduced from 0.8 to 0.3dB by design, *Figure 7*, [2].

The RF OE S21 performance of the waveguide detectors combined with the on-chip capacitors is shown in *Figure 8* for 3 different temperatures at maximum optical input power. The combined PD +CAP 3dB bandwidth is insensitive to temperature from -5 to 90C with a value of >32GHz.

#### 4. Fabrication and Manufacturability

Ridge waveguides are used on the InP PIC which benefit from high  $\Delta n$  enabling small bend radii. Low cost i-line lithography and ICP etching enables accurate representation of the design intent as can be seen from the SEM photo of the 4x4 MMI body shown in *Figure 9*.

Dimensional control of the 4x4 MMI is critical both for port balancing (CMRR) and loss over wavelength. In Figure 7 we show the modelled effect of fabricating a well centered MMI versus one centred  $\delta\lambda=+20\text{nm}$  too long, corresponding to a change of only 90nm in the critical width dimension for the non-wavelength flattened MMI [3]. At the  $\delta\lambda=+20\text{nm}$  and at extreme C-Band wavelengths, the standard MMI has a loss of -2.4dB compared with -1.06dB for the wavelength flattened MMI. In our PICs we have evaluated MMI centering over a number of designs and over a number of wafers.

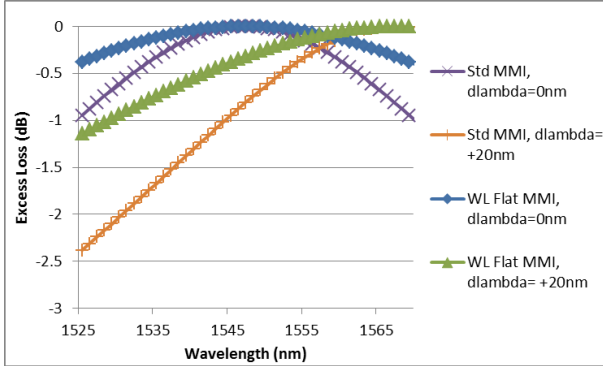


Figure 7 Modelled excess loss for standard and wavelength flat 4x4 MMI, with centre wavelengths  $1547.5\text{nm} + \text{dlambda}$ , where  $\text{dlambda}=0\text{nm} \ \& \ +20\text{nm}$

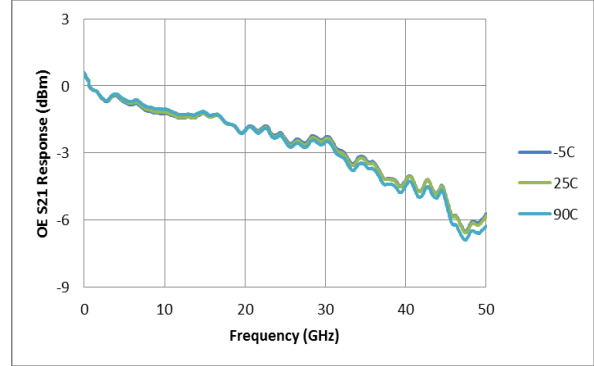


Figure 8 OE RF S21 response for waveguide detector and on-chip capacitor combined over temperature, worst case BW 32GHz

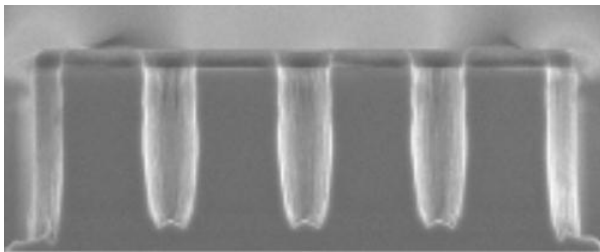


Figure 9 SEM showing 4x4 MMI body and access waveguides

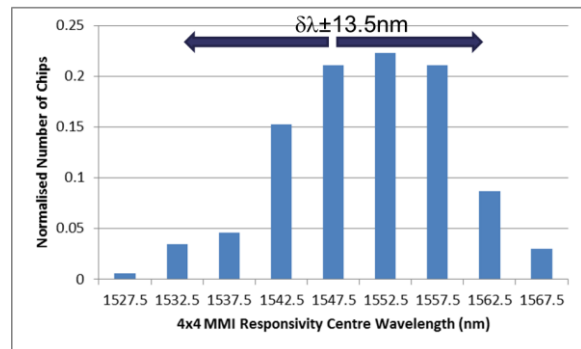


Figure 10 Centre wavelength spread in manufacturing of 4040 chips on multiple wafers is to 90% population,  $\delta\lambda \pm 13.5\text{nm}$

Figure 10 shows the spread in  $\delta\lambda$  achieved in manufacturing over 4000 chips and on multiple wafers; this includes a deliberate design spread across the wafer. If the  $\delta\lambda$  spread is attributed entirely to dimension control then 90% of the population of 4x4 MMI are within  $\delta\lambda = \pm 13.5\text{nm}$  or  $\delta W < \pm 61\text{nm}$ . On a wavelength flat MMI this corresponds to only 0.8dB absolute loss at the band extremes. In fact the fabrication tolerance on the width is  $\delta\lambda = \pm 10\text{nm}$  or  $\delta W = \pm 45\text{nm}$  on a single MMI design. We believe this demonstrates excellent manufacturability for this parameter.

## 5. Conclusion

Driven by requirements for wider deployment of 100G in metro networks via pluggable CFP2 modules, we report a miniaturized InP coherent receiver chip  $1.2 \times 3.33\text{mm}$  containing  $90^\circ$  hybrid and waveguide photodetectors with the highest reported responsivity  $0.151\text{A/W}$  simultaneously with 32GHz OE bandwidth response. The critical 4x4 MMI providing the  $90^\circ$  hybrid functionality is shown to be manufacturable to centre wavelength  $\delta\lambda = \pm 13.5\text{nm}$  or MMI width  $\delta W = \pm 60\text{nm}$  over more than 4000 devices. InP offers an attractive and manufacturable platform for size and cost reduction as well as a common platform for full transceiver (laser, Tx, Rx) integration.

## 6. References

- [1] Masaru Takechi et al, "Compact 100G Coherent Receiver Using InP-based  $90^\circ$  Hybrid Integrated with Photodiodes", ECOC 2013, P.2.8
- [2] Pierre A. Besse et al, "Optical Bandwidth and Fabrication Tolerances of Multimode Interference Couplers," JLT **12**, 1004-1009 (1994).
- [3] Lucas B. Soldano et al, "Optical Multi-Mode Interference Devices Based on Self-Imaging: Principles and Applications", JLT **13**, 615-627 (1995)